Sharp Roll-Off Ultra-Wide Stopband Compact Microstrip Lowpass Filter using Square-Shaped Resonator

Behnam Afzali[1]*, Farshid Yousefi Moghadam [2], Farshad Nadi[3], Rohallah Zallbeygi[4]
1,2,3,4- Department of Electrical Engineering, Faculty of Technical and Vocational No.2, Kermanshah Branch, Technical and Vocational University (TVU), Kermanshah, Iran.
Email: Behnam_Afzali66@yahoo.com (Corresponding author)
Email: Farshid_yosefi@yahoo.com, F.nadi@chmail.ir, Rohallah_zallbeygi@yahoo.com

Received: July 2018 Revised: October 2018 Accepted: December 2018

ABSTRACT:
In this paper, a novel compact microstrip Low-Pass Filter (LPF) with sharp roll-off and ultra-wide stopband with high suppression level is presented. In the proposed filter, square-shaped resonators are used. The cut-off frequency at 3dB is 1.88GHz. The maximum insertion loss of this filter is less than 0.1dB and the return loss is also less than 16dB in the passband. In the proposed structure, the stopband extends from 2.07 to 29.5 GHz at 24dB level of suppression and is considered as an ultra-wide stopband. There is a significant relationship between simulation and fabrication results, which have justified the functionality of the proposed LFP, respectively.

KEYWORDS: Cut-Off Frequency**,** Filter, LC Equivalent, Low-Pass, Microstrip, Resonator, Sharp Roll-Off, Square-Shaped, Transformation Function, Ultra-Wide Stopband.

1. INTRODUCTION

Microstrip lowpass filters are one of the most important elements in telecommunication systems. Filters essentially carry out two important actions in telecommunication systems: noise cancellation and separation of various frequency bands. Filters are used to select or curb RF/microwave signals according to what is needed. Their application includes wireless communications and RF/microwave filters which have high efficiency, small size and low light weight. [1], [2]. One of the techniques for designing a microstrip lowpass filter is using the DGS structure [3]. With the help of this structure, it is possible to design different resonators which generate zero transmissions in the stopband. However, this structure causes an undesirable sharp response in the passband. In recent years, multimode resonators [4] have been of interest to researchers because these resonators are very small, but the structure has disadvantages such as low attention level and high return loss. Using a compact microstrip resonant cell (CMRC), an ultra-wide stop band was investigated [5]. These resonators alone do not have a good performance in the stopband but if put together, they provide an ultra-wide stop bandwidth. The most important disadvantages of these resonators are large dimensions. Using lattice resonator, a microstrip lowpass filter has been designed [6], which has a sharp response in the transition band. Because of the high cut off frequency and inappropriate bandwidth, this filter is deprived of an optimal figure of merit. As seen in the design of this filter, a hairpin was used [7] which makes the stopband relatively suitable. But on the other hand, it caused a decrease in sharpness of the transition band, which reduces the figure of merit. Another filter was introduced using a hexagonal resonator and a DGS structure [8]. The transition zeros of this filter were constructed by using semicircular structures located in the ground plane. It is true that this filter has wide stop bandwidth, but insertion loss in the proposed structure is not acceptable, which also reduces the quality of the filter. One of the most important structures in the design of microwave circuits is the usage of a T-shaped structure [9]. With the help of the T-shaped structure, a sharp response can be created in the transition band. But on the other hand, if the T-resonator is used alone in the structure, it will cause a significant drop in return loss and increase insertion loss, due to the weaknesses in the design of the filter which has relatively large dimensions. Another method for designing a microstrip lowpass filter is to use a radial resonator [10]. This resonator provides a suitable cut-off frequency. By using curved lines, frequency response can be improved and stopband bandwidth can also be increased. A microstrip lowpass filter with wide bandwidth was studied by using rhombic resonators [11]. Rhombic resonators provide a very good attenuation level in the stopband but in the final filter

response, the filter does not have acceptable return loss and insertion loss and also suffers from a lack of sharp response in the transition band. In this paper, a novel microstrip LPF using square-shaped resonators, with an ultra-wide stopband from 2.07GHz to 29.5GHz at 24dB level of suppression is presented. Also, the proposed structure has an appropriate insertion loss and return loss in the passband. The proposed filter has very small dimensions of 0.18 λg* 0.14 λg, where λg is the guided wavelength at 1.88 GHz. The proposed LPF was simulated with the advanced design system (ADS) software and fabricated on a RO4003 substrate (εr=3.38, thickness = 32 mil and loss tangent 0.0021).

2. MAIN RESONATOR

The first step in designing a microstrip lowpass filter is the design of an ideal resonator, with the appropriate transmission zeroes in the stopband. As shown in Fig. 1, T-shaped and square-shaped resonators were combined to improve the frequency response in the passband, generate strong transition zeroes at various frequencies to achieve wide stopband and proper return and insertion losses. All of these combinations were designed to achieve a comprehensive resonator to resolve all the weaknesses of the parameters. The calculated dimensions for the layout of the main resonator are: L1 = 9.1mm, L2 = 1mm, L3 = 1.5, W1 = 0.1mm, W2 = 0.3, W3 = 2.95mm, W4 = 2.85mm, W5 = 2.4mm, W6 = 0.55mm.

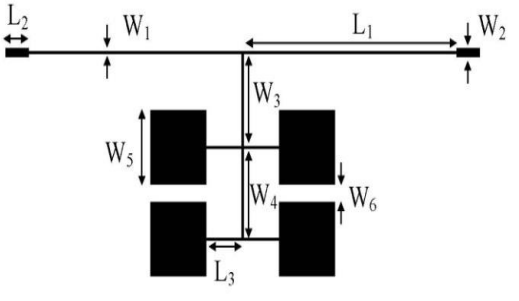

Fig. 1. Layout of the main resonator.

The following models and relationships were used to extract the LC equivalent resonator. The values of those parameters can be extracted using methods discussed in (1, 2), a high-and low-impedance lossless line terminated at both ends by relatively low impedance lines as shown in Fig. 2(a) which could also be presented by a π-equivalent circuit, as shown in Fig. 2(b).

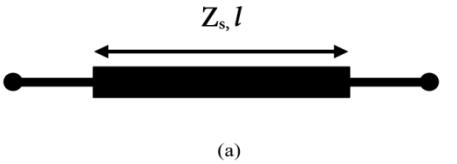

(a)

Fig. 2. (a) Layout of high-and low-impedance Lossless line.

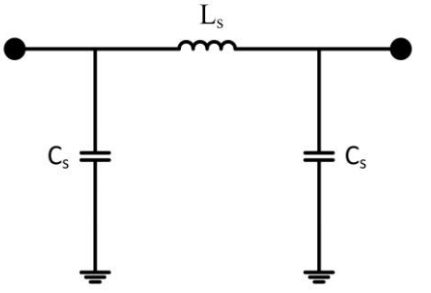

(b)

Fig. 2. (b) LC equivalent circuit.

The values of inductors and capacitors can be obtained as:

$$L_S = \frac{1}{\omega} * z_S * \sin\left(\frac{2\pi}{\lambda_g} l\right) \quad (1)$$

$$C_S = \frac{1}{\omega} * \frac{1}{z_S} * \tan\left(\frac{\pi}{\lambda_g} l\right) \quad (2)$$

Where, z_s is the characteristic impedance of the line; l is its length and λ_g is the guided wavelength at the cut off frequency. Formulas of open-end were discussed in [1]. Also, the structure and equivalent circuit are shown in Fig. 3(a-b).

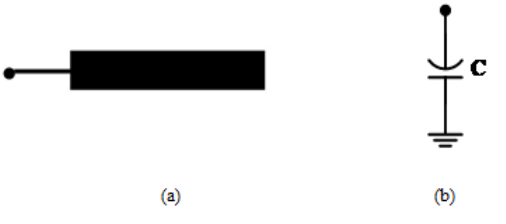

(a) (b)

Fig. 3. (a) layout of the open-end, (b) LC equivalent circuit.

The equivalent LC circuit (Fig. 4) of the main resonator was designed according to the models presented in Figs. 2 and 3. The quantities of inductors and capacitors in the LC equivalent was designed and calculated according to equations 1 and 2. The values of these parameters are presented in Table 1.

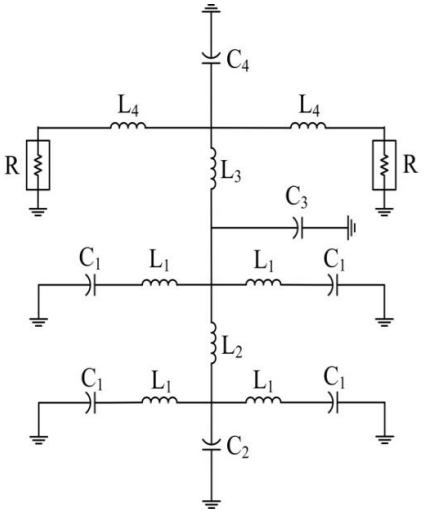

Fig. 4. LC equivalent of main resonator.

Table 1. Calculated indicators and capacitors.

Parameters	L_1	L_2	L_3	L_4
Value	1.23nH	2.37nH	2.37nH	5.6nH
Parameters	C_1	C_2	C_3	C_4
Value	0.39pF	0.09pF	13pF	0.27pF

The transformation function was expressed according to the equivalent LC circuit of the extracted resonator, as follows. With the help of this transformation function and changing the values of the inductor and the capacitor, we can shift the cutoff frequency. As shown in equations (1) and (2), changing the values of inductors and capacitors by changing the length and thickness of the microstrip lines is easily possible.

$$\frac{V_o}{V_i} = \frac{CR}{(R+L_4S)(2C+R+L_1S)} \quad (3)$$

$$C = \frac{1+BC_4S+C_4L_3S^2}{C_4S} \quad (4)$$

$$B = \frac{1+2AL_2S+C_2L_2S^2}{4A+C_2S+C_3S+4A^2L_2S+2AC_2L_2S^2+2AC_3L_2S^2+C_2C_3L_2S^3} \quad (5)$$

$$A = \frac{C_1S}{1+C_1L_1S^2} \quad (6)$$

Where, R is the matching impedance and its value is 50 ohms.

The frequency response of the proposed resonator with the LC equivalent circuit response is shown in Fig. 5. A significant relationship was shown between the frequency response of the proposed resonator and LC equivalent circuit response. The transmission zeros of this resonator were produced at frequencies of 2.163 and 4.546 GHz with values of -51.93 and -39.952 dB, respectively. The proposed response was similar to the response of a microstrip lowpass filter, but the return loss in the stopband at 4.212 and 8.36 GHz were very inadequate. To completely solve this problem, another resonator can be designed.

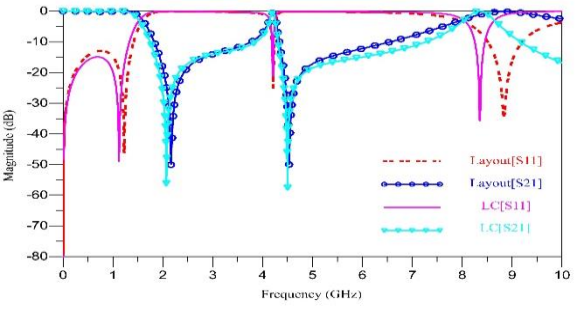

Fig. 5. Frequency response of the main resonator and LC equivalent circuit.

3. SECOND RESONATOR

With the help of the modified L-shaped structure shown in Fig. 6, a new resonator was designed to improve frequency response. The calculated parameters for the modified L-shaped were as follows: L_4 = 5.2mm, L_5 = 3.5mm, W_7 = 6.9mm, W_8 = 0.3mm. The LC equivalent circuit of the proposed resonator is shown in Fig. 7. Table 2 shows the quantities of inductors and capacitors.

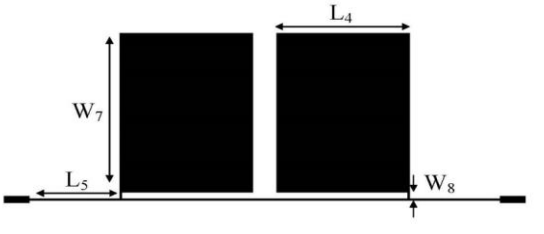

Fig. 6. Layout of the second resonator.

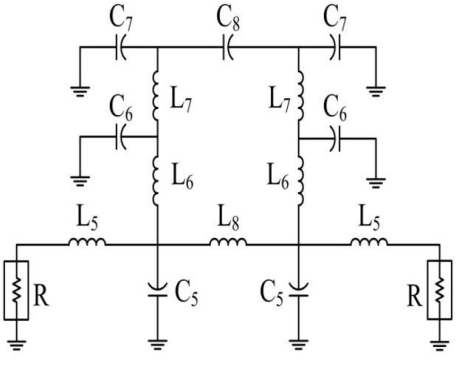

Fig. 7. LC equivalent circuit.

Table 2. Calculated indicators and capacitors of the LC equivalent second resonator.

Parameters	L_5	L_6	L_7	L_8
Value	1.72nH	0.2nH	58nH	8.45nH
Parameters	C_5	C_6	C_7	C_8
Value	22pF	0.4pF	1.36pF	0.02pF

As shown in the frequency response of the proposed resonator in Fig. 8, the transmission zeros of this resonator were produced at frequencies of 3.233 and 4.792 GHz with values of -51.129 and 50.952 dB, respectively. This modified L-shaped resonator provides a good stopband with a high attenuation level. The frequency response of the proposed resonator, along with the frequency response of the LC equivalent circuit is shown in Fig. 8.

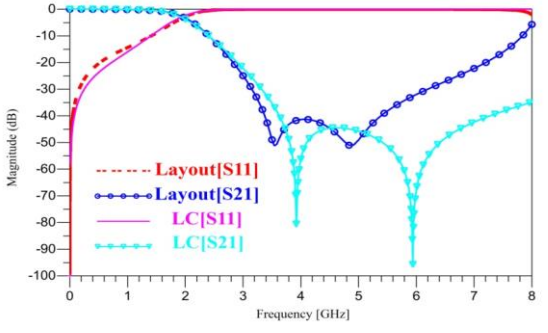

Fig. 8. Frequency response of the second resonator and LC equivalent circuit.

To achieve a suitable frequency response, the main resonator with modified L-shaped resonator should be combined. The structure of the proposed combined resonators is shown in Fig. 9 and the results of the combination are presented in Fig. 10.

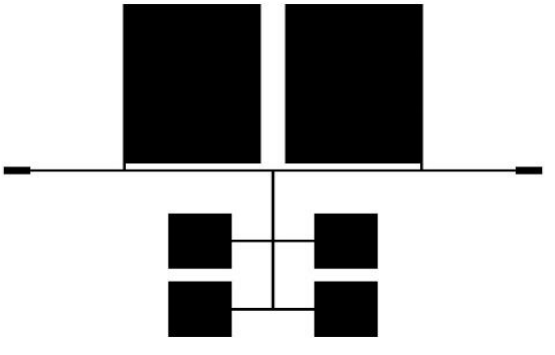

Fig. 9. Structure of the combined resonators.

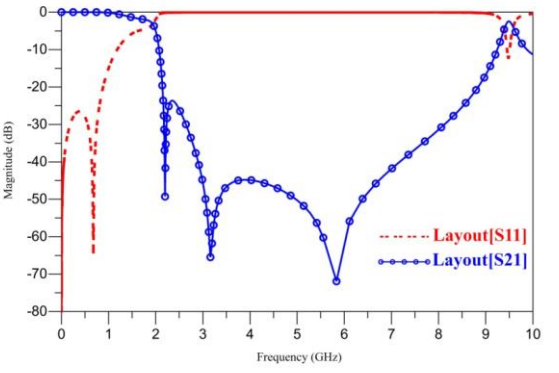

Fig. 10. Frequency response of the combination.

4. STUB DESIGN

According to the results presented in Fig. 10, the stopband bandwidth was greatly improved, but the frequency response could still be much better. By adding two stubs to both sides of the filter, an ultra-wide stopband can be achieved with excellent insertion loss in the passband. The dimensions of the stubs were as follows: L6 = 0.9mm, L7 = 0.5mm, L8 = 0.7mm, L9 =0.9mm, L10 = 0.5mm, W9 = 5.4, W10 = 2.9mm.

The structure of the proposed stubs, along with the resonators is shown in Fig. 11, and the final results of the frequency response, are shown in Fig. 12.

As seen in Fig. 12, the combination of all structures, including T-shaped, square- shaped and modified L-shaped resonators with stubs provided an ideal microstrip lowpass filter with all the parameters including sharpness response in the transition band, ultra-wide stopband with high suppression level and very suitable insertion and return losses.

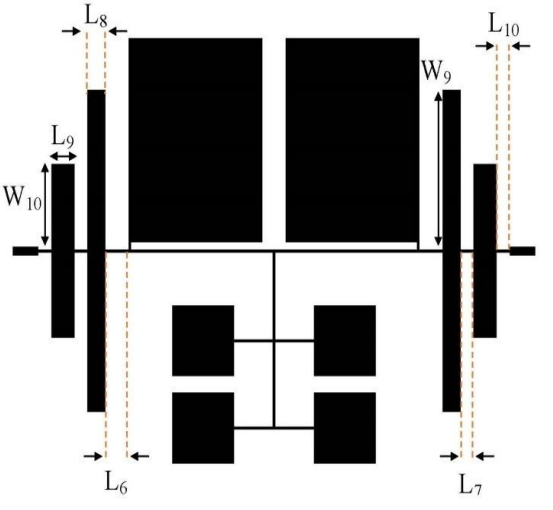

Fig. 11. Final structure of the filter.

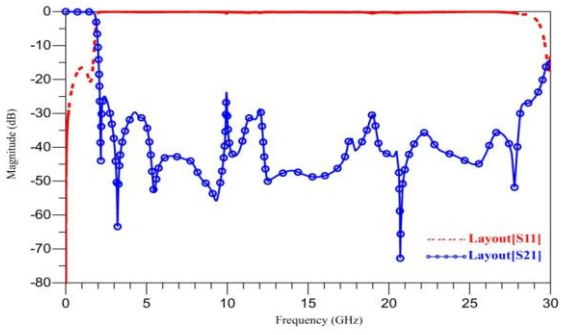

Fig. 12. Final frequency response of the ultimate structure.

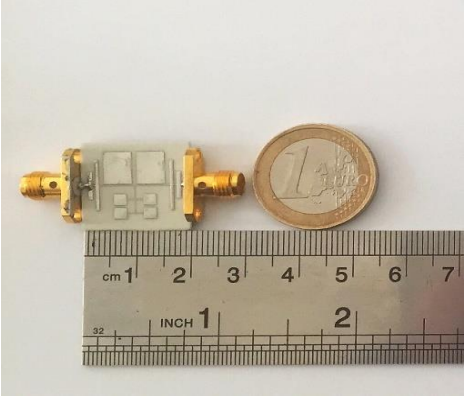

Fig. 13. Fabricated filter.

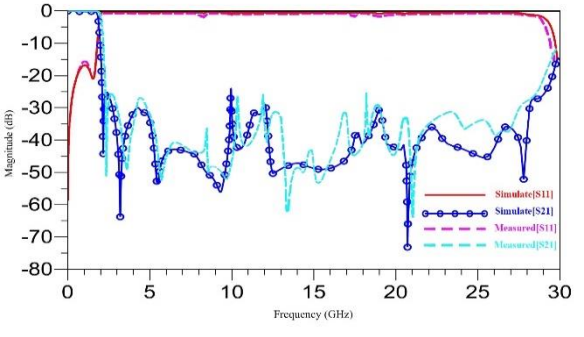

Fig. 14. Frequency response of the fabricated filter.

5. SIMULATION AND MEASUREMENT RESULT

The final filter, shown in Fig. 11, was fabricated on a 32-mil thick RO4003 substrate with a relative dielectric constant of 3.38 and loss tangent of 0.0021 (Fig. 13). The dimensions of the fabricated filter were about 18.3 mm× 14.4 mm, which corresponds to an electrical size of $0.18\lambda_g \times 0.14\ \lambda_g$, where λ_g is the guided wavelength at 1.88 GHz. Also, as seen in Fig. 14, there is a significant relationship between simulation and measurement.

Sharpness in the transition band is calculated using Equation 7, as follows:

$$\varepsilon = \frac{\alpha_{max} - \alpha_{min}}{f_s - f_c} \quad (7)$$

where, α_{max} is the -40dB attenuation point, α_{min} is the -3dB attenuation point, f_s is -40dB stopband frequency, and f_c is the -3dB cut-off frequency. The relative stopband bandwidth is calculated by:

$$RSB = \frac{\text{Stopband bandwidth}}{\text{Stopband center frequency}} \quad (8)$$

The suppression level (SF) is defined as:

$$SF = \frac{\text{Rejection level in stopband}}{10} \quad (9)$$

The normalized circuit size (NCS) is as follows:

$$NCS = \frac{\text{Physical Size (Length*Width)}}{\lambda_g^2} \quad (10)$$

Where, λ_g is the guided wavelength and is calculated by:

$$\lambda_g = \frac{300}{f_c\sqrt{\varepsilon_{re}}} \quad (11)$$

Finally, using all of the above equation, the figure of merit was calculated as follows:

$$FOM = \frac{\varepsilon * RSB * SF}{NCS * AF} \quad (12)$$

Table 3. (a) Performance comparison of the proposed filter with other filters.

Refs.	F_c (GHz)	Roll-off	RL (dB)	IL (dB)
3	2.45	56.7	17	0.3
4	1.8	17	10	0.5
5	1.5	97.4	15	0.1
6	4.34	100	19	0.1
7	1.6	52.8	20	0.3
8	2.45	100	18	0.85
9	1.26	217	9	0.8
12	0.5	95	16.3	0.5
13	1.71	100	18	0.1
14	2.8	48.5	16.5	0.1
15	3.14	70	13	0.28
16	2.28	122	12.3	0.37
17	3.37	188	10	0.83
18	2.97	84.69	18.7	0.06
19	2.28	94	21	0.3
20	1.53	29.3	20	0.1
21	2	43.9	10	1
22	3.09	46	10	0.5
23	5.15	103	10	0.1
24	3.8	26	14	0.1
Proposed filter	1.88	137	16	0.1

Table 3. (b) Performance comparison of the proposed filter with other filters.

Refs.	NCS (λ_g^2)	SF	AF	RSB	FOM
3	0.115 * 0.116	2	2	1.63	7109
4	0.09 * 0.11	1.5	1	1.58	4476
5	0.1 * 0.19	2	1	1.87	19172
6	0.67 * 0.11	2	1	1.58	4328
7	0.081 * 0.113	2	1	1.52	18475
8	0.255 * 0.131	2	2	1.49	9030
9	0.12 * 0.29	2	1	1.65	19931
12	0.214 * 0.104	2	1	1.4	11951
13	0.21 * 0.09	1.6	1	1.71	13680
14	0.141 * 0.151	2	1	1.61	7436
15	0.166 * 0.147	1	2	1.4	1200
16	0.137 * 0.247	2	1	1.44	10647
17	0.2 * 0.18	2	1	0.9	9400
18	0.143 * 0.156	2	1	1.51	11625
19	0.243 * 0.169	2.3	1	1.26	6645
20	0.15 * 0.05	2.4	2	1.53	7172
21	0.101 * 0.15	1	1	1.63	4771
22	0.22 * 0.13	2	1	1.37	4502
23	0.34*0.18	2	1	1.56	5269
24	0.18*0.1	2	1	1.34	3872
Proposed filter	0.18 * 0.14	2.4	1	1.74	22884

As shown in Table 3 (a, b), the performance of this filter including sharpness in transition band, insertion loss, return loss, suppression factor, normalized circuit size (NCS), relative stopband bandwidth (RSB) and figure of merit (FOM) were compared with others.

6. CONCLUSION

A microstrip lowpass filter using square-shaped resonators was designed and fabricated. This filter had ultra-wide stopband of between 2.07 to 29.5GHz with 24dB level of suppression. Also, the maximum insertion loss was< 0.1dB and return loss was<16dB. The size of the filter was $0.18\lambda_g$* $0.14\ \lambda_g$ which was very small. The fabricated filter had a very suitable sharpness in the transition band. These filters are widely used in modern telecommunications to remove additional harmonics and unwanted signals in modern communication systems such as mobile communication systems, and satellites.

7. ACKNOWLEDGMENT

The authors would like to thank the Technical and Vocational University (TVU), Kermanshah Branch, Faculty of Technical and Vocational No.2 for the technical support.

REFERENCES

[1] D. M. Pozar, **"Microwave Engineering,"** *Wiley, New York*, 2005.

[2] [2] Hong, J. S. and Lancaster, M. J. **"Microstrip Filters for RF/Microwave Applications,"** *New York: Wiley*, 2001.

[3] S. Jiang, J. Xu, **"Compact Microstrip Lowpass Filter With Ultra-Wide Stopband Based on Dual-Plane Structure,"** *Electronics Letters*, Vol. 53(9), pp. 607-609, 2017.

[4] Q. Li, Y. Zhang, Y. Fan, **"Compact Ultra-Wide Stopband Lowpass Filter Using Multimode Resonators,"** *Electronics Letters*, Vol. 51(14). pp. 1084-1085, 2015.

[5] S. Roshani**, "A Compact Microstrip Low-Pass Filter With Ultra-Wide Stopband Using Compact Microstrip Resonant Cells,"** *International Journal of Microwave and Wireless Technologies*, Vol. 9(5), pp. 1023-1027, 2017.

[6] [6] M. Hayati, M. Ekhteraei, F. Shama, **"Compact Lowpass Filter With Flat Group Delay Using Lattice-Shaped Resonator,"** *Electronics Letters*, Vol. 53 (7), pp. 475 – 476, 2017.

[7] S. Liu, J. Xu, Z. Xu, **"Compact Lowpass Filter With Wide Stopband Using Stepped Impedance Hairpin Units,"** *Electronics Letters*, Vol. 51(1), pp. 67-69, 2015.

[8] L. Kumar, M.S. Parihar, **"Compact Hexagonal Shape Elliptical Lowpass Filter With Wide Stop Band,"** *IEEE Microwave and Wireless Components Letters*, Vol. 26(12), pp. 978-980, 2016.

[9] G. Karimi, A. Lalbakhsh, H. Siahkamari, **"Design of Sharp Roll-Off Lowpass filter with Ultra-Wide Stopband,"** *IEEE Microwave and Wireless Components Letters*, Vol. 23(6), pp. 303–305, 2013.

[10] M. Hayati, M. Khodadoost, H. Abbasi, **"Microstrip Lowpass Filter With Wide Stopband and Sharp Roll-Off Using Modified Radial Stub Resonator,"** *International Journal of Microwave and Wireless Technologies*, Vol. 9(3), pp. 499- 504, 2017.

[11] B, Zhang, S. Li, J. Huang, **"Compact Lowpass Filter With Wide Stopband Using Coupled Rhombic Stubs,"** *Electronics Letters*, Vol. 51(3), pp. 264-266, 2015.

[12] V.K Velidi, S. Sanyal, **"Sharp Roll-Off Low Pass filter with Wide Stopband Using Stub-Loaded Coupled-Line Hairpin Unit,"** *IEEE Microwave and Wireless Components Letters*, Vol. 21(6), pp. 301–303, 2011.

[13] S. Majidifar, **"High Performance Microstrip LPFs Using Dual Taper Loaded Resonator,"**

International Journal for Light and Electron Optics, Vol. 127(6), pp. 3484–3488, 2016.

[14] A. Sheikhi, A. Alipour, H. Hemesi, **"Design of Microstrip Wide Stopband Lowpass Filter With Lumped Equivalent Circuit,"** *Electronics Letters*, Vol. 53(21), pp. 1416-1418, 2017.

[15] A. Faraghi, M. Ojaroudi, N. Ghadimi, **"Compact Microstrip Low-Pass filter with Sharp Selection Characteristics Using Triple Novel Defected Structures for UWB applications,"** *Microwave and Optical Technology Letters*, Vol. 56(4), pp.1007–1010, 2014.

[16] S.V Makki, A, Ahmadi, S, Majidifar, H, Sariri, Z. Rahmani, **"Sharp Response Microstrip LPF using Folded Stepped Impedance Open Stubs,"** *Radio engineering*, Vol. 22(1), pp. 328-332, 2013.

[17] M. Xiao, G. Sun, X. Li, **"A Lowpass Filter with Compact Size and Sharp Roll-Off,"** *IEEE Microwave and Wireless Components Letters*, 25(12): 790-792, 2015.

[18] M. Hayati, M. Gholami, H.S. Vaziri, T. Zaree, **"Design of Microstrip Lowpass filter with Wide Stopband and Sharp Roll-Off Using Hexangular Shaped Resonator"** *Electronics Letters*, Vol. 51(1), pp. 69–71, 2014.

[19] P.M. Raphika, P. Abdulla, P.M. Jasmine, **"Planar Elliptic Function Lowpass Filter with Sharp Roll-Off and Wide Stopband,"** *Microwave and Optical Technology Letters*, Vol. 58(1), pp. 133-136, 2016.

[20] S. Majidifar, **"Design of High Performance Miniaturized Lowpass Filter Using New Approach of Modeling,"** *Applied Computational Electromagnetics Society Journal*, Vol. 31(1), pp. 52-57, 2016.

[21] F. Wei, L. Chen, X.W. Shi, **"Compact Lowpass Filter Based on Coupled-Line Hairpin Unit,"** *Electronics Letters*, Vol. 48(7), pp.379-381, 2012.

[22] H. Sariri, Z. Rahmani, A. Lalbakhsh, S. Majidifar, **"Compact LPF using T-shaped resonator,"** *Frequenz*, Vol. 67(1–2), pp. 17–20, 2013.

[23] A. Kolahi, F. Shama, **"Compact Microstrip Low Pass Filter With Flat Group-Delay Using Triangle-Shaped Resonators,"** *International Journal of Electronics and Communications (AEU)*, Vol. 83, pp. 433-438, 2018.

[24] B. Hiedari, F. Shama, **"A Harmonics Suppressed Microstrip Cell for Integrated Applications,"** *International Journal of Electronics and Communications (AEU)*, Vol. 83, pp. 519-522, 2018.